Journal of Bionic Engineering (2023) 20:2661–2669
https://doi.org/10.1007/s42235-023-00415-0

RESEARCH ARTICLE

All-Fabric Bi-directional Actuators for Multi-joint Assistance of Upper Limb

Junlin Ma[1] · Diansheng Chen[1] · Zhe Liu[1] · Jie Wei[1] · Xianglin Zhang[1] · Zihan Zeng[1] · Yongkang Jiang[2,3]

Received: 15 February 2023 / Revised: 28 June 2023 / Accepted: 30 June 2023 / Published online: 2 August 2023

Abstract
According to clinical studies, upper limb robotic suits are vital to reduce therapist fatigue and accelerate patient rehabilitation. Soft pneumatic actuators have drawn increasing attention for the development of wearable robots due to their low weight, flexibility, and high power-to-weight ratio. However, most of current actuators were designed for the flexion assistance of a specific joint, and that for joint extension requires further investigation. Furthermore, designing an actuator for diverse working scenarios remains a challenge. In this paper, we propose an all-fabric bi-directional actuator to assist the flexion and extension of the elbow, wrist, and fingers. A mathematical model is presented that predicts the deformation and guides the design of the proposed bi-directional actuator. To further validate the applicability and adaptability of the proposed actuator for different joints, we developed a 3-DOF soft robotic suit. Preliminary results show that the robotic suit can assist the motion of the elbow, wrist, and finger of the subject.

Keywords Soft robotic suits · Fabric-based actuators · Multi-DOF motion · Upper limb rehabilitation

1 Introduction

Strokes are a common cause of long-term upper limb disability. Approximately 80% of stroke survivors suffer upper limb dysfunction, severely affecting their daily lives [1]. Medical research has shown that this group of patients can accelerate their upper extremity rehabilitation by rebuilding neurological function in the brain through extensive repetitive motion [2]. However, most existing upper limb rehabilitation training is performed manually by physicians, making the process labor-intensive, time-consuming, and expensive. With the development of rehabilitation robotics, many researchers have proposed a rigid exoskeleton [3–5]. These exoskeletons have a rigid frame aligned with the upper limb skeleton and can precisely assist with complex movements of the upper limb joints. However, the exoskeleton has a bulky structure, is incompatible with human movement, and can cause discomfort due to its complex system and rigid frame.

Consequently, some researchers have developed frameless soft robotic suits that are structurally lightweight, compliant, and comfortable [6]. These suits made using compliant materials, such as cables [7–9], elastomers [10–12], and textiles [13], are purported to be clothing-like robots that wrap around the body and work in parallel with muscles.

Among these, textile actuators have contributed to rapid developments in soft wearable devices owing to their foldability, flexibility, zero initial stiffness, and high power-to-weight ratio. O'Neill et al. [14–16] designed fabric pneumatic actuators to assist shoulder abduction. Thalman [17] used multiple rectangular fabric actuators arranged along a non-extendable fabric for elbow flexion assistance. Park et al. [18] and Realmuto et al. [19] proposed flat and helical pneumatic actuators to assist forearm pronation and supination, respectively. Bartlett [20] presented a soft device for wrist flexion and extension.

✉ Diansheng Chen
chends@163.com

[1] Institute of Robotics, Beihang University, Beijing 100191, China

[2] Department of Control Science and Engineering, Tongji University, Shanghai 201804, China

[3] Frontiers Science Center for Intelligent Autonomous Systems, Shanghai 201210, China

Researchers [13, 21, 22] have designed different actuators to assist various upper limb joints. However, most studies [16–18, 23] focused on flexion assistance in only one upper extremity joint. Some studies [24] focus on assisting two joints but usually use different actuator structures, which is poorly generalized for other joints. In addition, most studies simplify the modeling by cylindrical and prismatic assumptions [25–27]. There are fewer studies on actuator deformation. Hence, designing an actuator for multi-joint bi-directional assistance remains challenging.

This study proposes a fabric-based bi-directional actuator that can assist the flexion and extension of the elbow, wrist, and finger. We also provide a mathematical model to predict the deformation and output torque, and this model further guides actuator parameter design. We determined the geometric parameters of the actuators based on the required torque and motion range for the flexion/extension of the elbow, wrist, and fingers in adults. Furthermore, we characterized the effect of the input pressure and initial angle on the output torque and validated the theoretical model. Additionally, we developed a 3-DOF soft robotic suit based on the proposed bi-directional actuator. Preliminary results demonstrate that the suit can assist with elbow, wrist, and finger flexion/extension. The main contributions of this study are as follows:

(1) Proposal of a fabric-based bi-directional actuator to assist the elbow, wrist, and finger flexion/extension.
(2) Modeling, validation, and characterization of the proposed actuator.
(3) Integration of a 3-DOF soft robotic suit, including elbow, wrist, and finger flexion/extension.

2 Actuator Design, Modeling, and Characterization

2.1 Actuator Design and Fabrication

Unlike the existing actuators that focus on either flexion or extension assistance of a single joint of a human's upper limb, such as the elbow [17], wrist [20], and fingers [13], the proposed actuator uses bending and straightening bladders to achieve bi-directional motion, as shown in Fig. 1a. The bending and straightening bladders are mounted on the dorsal and ventral sides for flexion and extension, respectively. Figure 1b demonstrates that the actuator can adapt to different upper limb joints (elbow, wrist, and fingers) by simply changing the structural parameters.

The above-mentioned flexion and extension actuators are derived from fabric bladders. The bladder comprises two pieces of composite textile. Each composite fabric contains two thin layers: a hot-melt material and stretch-resistant flexible material, as shown in Fig. 2a. In this study, we chose thermoplastic polyurethane (TPU)–fabric composite as the hot-melt and stretch-resistant flexible material, respectively.

The fabrication of the fabric bladder is as follows. First, the two TPU–fabric composites were stacked: one on top of the other, to obtain a total thickness of 0.24 mm. We then laser-cut the desired TPU–fabric shape (shown as a rectangle here). Second, we placed an aluminum alloy of the same shape and size as a mold above the two TPU–fabric pieces (the mold has a thickness of 2 mm, a rectangular border shape, and a gap at one end for inserting the air tube). Next, a polyimide sheet was placed near the inner edge of the mold as a thermal barrier to prevent internal adhesion. To further ensure the consistency of the bladder, a spacer was placed between the two layers to

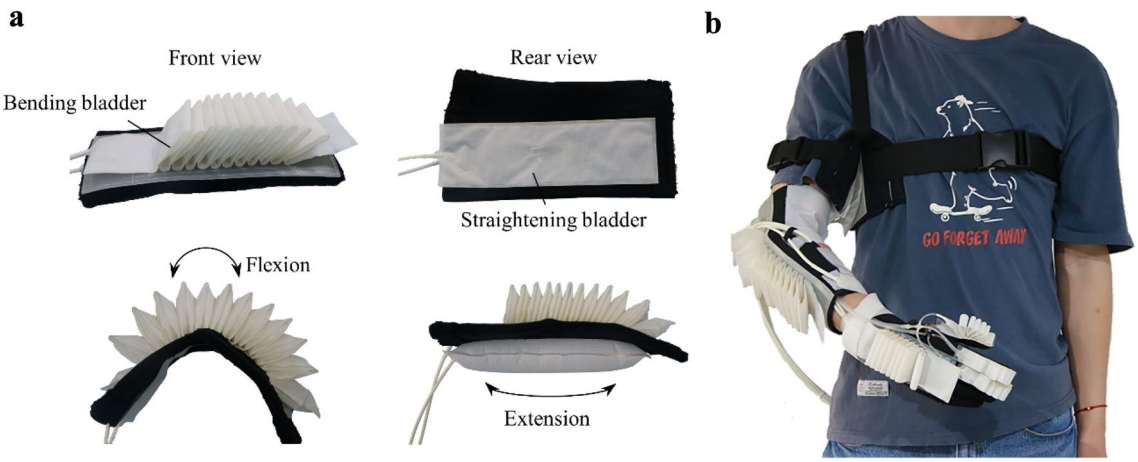

Fig. 1 **a** Structure of the fabric-based bi-directional actuator. The actuator bends when the bending bladder is pressurized, and the actuator straightens when the straightening bladder is inflated. **b** Bi-directional actuators for elbow, wrist, and finger, integrated into a 3-DOF soft robotic suit

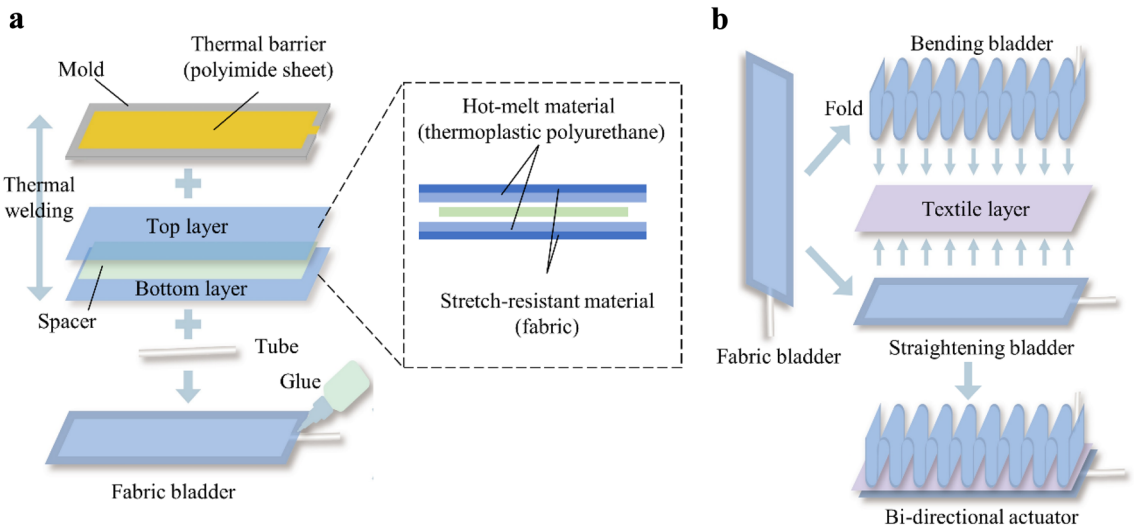

Fig. 2 Components and fabrication of the fabric-based bi-directional actuator. **a** The main fabrication process of the fabric bladder and **b** assembly of the bi-directional actuator

isolate the top and bottom layers. Finally, the two pieces of TPU–fabric composite were heat-pressed at 200 °C to form a cavity pocket with a gap; the air tube was inserted at the hole and sealed with glue.

After inflating the internal air cavity, the fabric bladder expands and deforms into a shape similar to a pillow. If the bladder folds in half, its inflation and expansion will straighten and actuator stiffen axially; this is called the straightening bladder. Alternatively, if we lengthen and fold the fabric bladder into a corrugated shape, we obtain the bending bladder. The straightening and bending bladders were connected with a piece of textile, as shown in Fig. 2b, to fabricate the bi-directional actuator.

2.2 Actuator Modeling

We first studied the deformation–pressure characteristics to quantify the mechanical properties of the bi-directional actuators. Furthermore, we investigated the effects of input pressure and initial angle on the output torque of the actuator.

First, we analyzed the actuator flexion motion, as shown in Fig. 3a. Only the elbow is shown here as the wrist and fingers also use the same structure. We selected one of the lamellae as the object and established a three-dimensional coordinate system with center O of the layer as the origin (y-direction is inwardly perpendicular to the paper face). According to Timoshenko's large deformation theory [28], the deflection of the actuator after deformation is as follows:

$$z = a_{00}\left(a^2 - x^2\right)\left(b^2 - y^2\right), \tag{1}$$

where a and b are half the length and width of the thin layer, respectively. We use (u, v) to denote the strain in the (x, y) direction, because the deformation of the actuator leads to non-negligible stretching in the plane. Based on [28], we describe the thin-layer deformation function as follows:

$$\begin{aligned} u &= x\left(b_{00} + b_{10}x^2 + b_{01}y^2 + b_{11}x^2y^2\right) \\ v &= y\left(c_{00} + c_{10}x^2 + c_{01}y^2 + c_{11}x^2y^2\right), \end{aligned} \tag{2}$$

where $a_{00}, b_{ij}, c_{ij}, (i,j = 0, 1)$ are the parameters of the system of equations that require solving. The strain energy V within the thin layer after deformation consists of the following two components:

$$V = V_b + V_e, \tag{3}$$

where V_b is the bending strain energy due to pure bending and V_e is the tensile strain energy due to elongation within the neutral plane. From the principle of virtual displacement, it follows that:

$$\delta V - \delta \iint qz dx dy = 0, \tag{4}$$

where q is the pressure inside the actuator. Jointly, Eqs. (2–4) lead to

$$\begin{aligned} &Q = V - \iint qz\mathrm{d}x\mathrm{d}y\frac{\partial Q}{\partial a_{00}} = 0; \\ &\frac{\partial Q}{\partial b_{ij}} = 0; \frac{\partial Q}{\partial c_{ij}} = 0. \quad i,j = 0, 1. \end{aligned} \tag{5}$$

Equation (5) is a set of nine nonlinear equations containing the coefficients $a_{00}, b_{ij}, c_{ij}, (i,j = 0, 1)$. Upon solving this set of equations, we can obtain all coefficients. The values

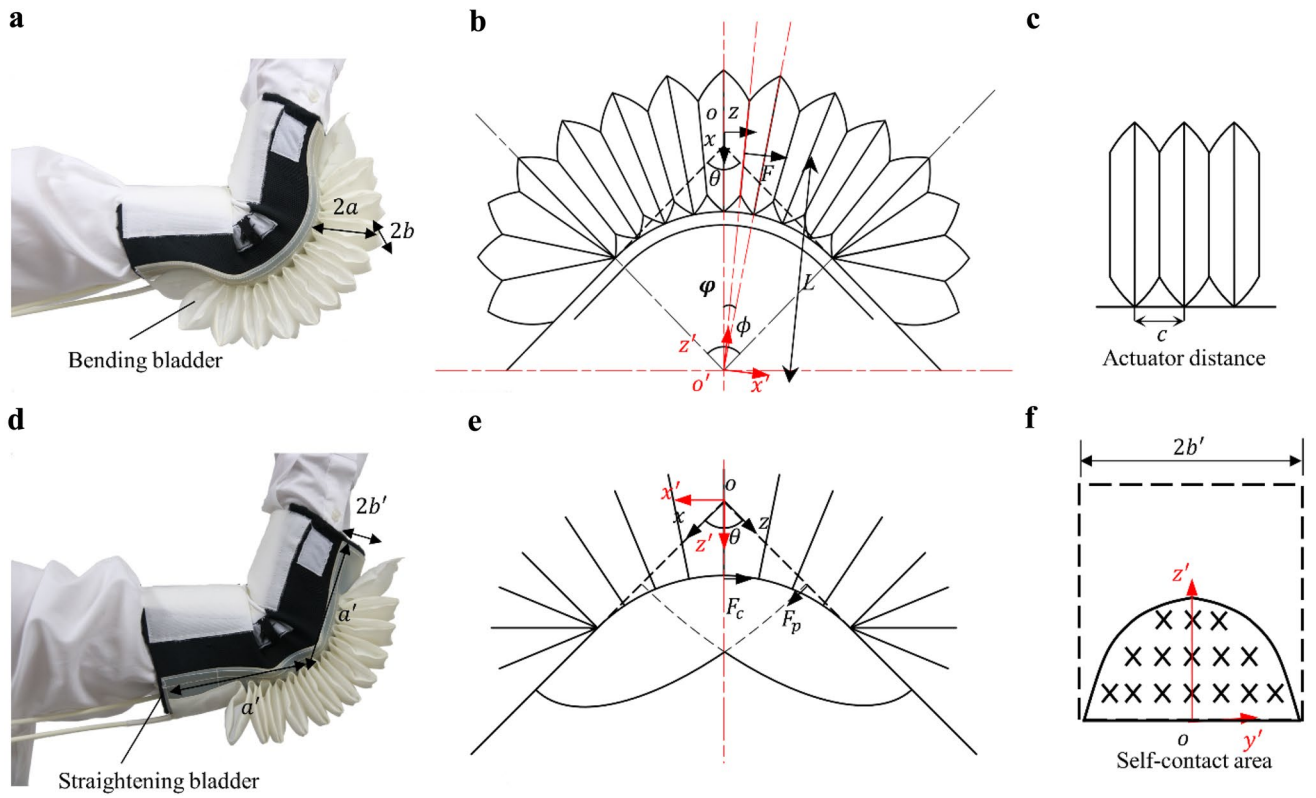

Fig. 3 Mathematical model of the actuators. **a** Flexion of the actuator on the elbow. **b** Force analysis and boundary conditions for flexion of the actuator. Consider the middle part adjacent to the two pieces of the actuator contact force. The deformation of each side of the follows: Eq. (2), but only half along the length direction, similar to half a pillow, **c** adjacent actuator distance before bending, **d** extension of the actuator on the elbow, **e** force analysis and boundary conditions for extension of the actuator, and **f** actuator self-contact region

are substituted in Eq. (1) to obtain the deformation function of the actuator.

Subsequently, we created a flexion torque expression (Eq. (6)), where S represents the contact area of the adjacent layers and L is the length of the force arm; N is the number of thin layers and $n = N - 6$ is the number of layers involved in bending; θ is the bending angle of the actuator and c is the distance between adjacent actuators (Fig. 3c)

$$M = PSL \tag{6}$$

$$L = \frac{(n-1)c}{\phi} + a \tag{7}$$

$$\frac{\varphi}{2} = \frac{\phi}{2(n-1)} = \frac{\pi-\theta}{2(n-1)}. \tag{8}$$

Moving the coordinate system xyz-0 along the x-axis by length L and rotating $\frac{\pi-\varphi}{2}$ counterclockwise around the y-axis to $x'y'z'-O$, we obtain

$$z\prime = x\cos\frac{\varphi}{2} + a_{00}\left(a^2 - x^2\right)\left(b^2 - y^2\right)\sin\frac{\varphi}{2} - L\cos\frac{\varphi}{2}. \tag{9}$$

Let $x = 0$. Then, the actuator self-contact range is expressed as

$$S\int_{-b}^{b}\left[\begin{array}{c} a_{00}a^2\left(b^2 - y^2\right)\sin\frac{\pi-\theta}{2(n-1)} \\ +L\cos\frac{\pi-\theta}{2(n-1)} \end{array}\right]\mathrm{d}y. \tag{10}$$

Finally, we can obtain the expression for the flexion torque:

$$\begin{aligned} M = P\left[\frac{(n-1)c}{\pi-\theta} + a\right] * \\ \left[\frac{4}{3}a_{00}a^2b^3\sin\frac{\pi-\theta}{2(n-1)} + 2bL\cos\frac{\pi-\theta}{2(n-1)}\right]. \end{aligned} \tag{11}$$

Furthermore, for the joint extension (Fig. 3d), we also developed a torque expression conditioned on geometric parameters, internal pressure $P\prime$, and bending angle θ

$$M\prime = F_p \frac{a\prime}{2} \tag{12}$$

$$F_p = F_c \cos\frac{\theta}{2} \tag{13}$$

$$F_c = P\prime S\prime. \tag{14}$$

Here, a' is half the length of the straightened bladder, b' is half the width, and S' is the self-contact area of the actuator. As shown in Fig. 3e, we establish $xyz{-}O$ at the center of the actuator before deformation. By rotating the coordinate system $xyz - O$ by $\theta/2$ along the y-axis to $x'y'z' - O$, we obtain the following according to the coordinate transformation:

$$z\prime = -x\sin\theta + a_{00}\left(a\prime^2 - x^2\right)\left(b\prime^2 - y^2\right)\cos\frac{\theta}{2}. \tag{15}$$

Let $x = 0$. Then, the actuator self-contact range is expressed as

$$S\prime = \int_{-b}^{b} a_{00} a\prime^2 \left(b\prime^2 - y^2\right)\cos\frac{\theta}{2}\mathrm{d}y. \tag{16}$$

Finally, we can obtain the expression for the extension torque

$$M\prime = \frac{2}{3} a_{00} a\prime^3 b\prime^3 P'^{\cos\frac{\theta}{2}\cos\frac{\theta}{2}}. \tag{17}$$

2.3 Characterization

To determine the geometrical parameters of different joint actuators, we referred to the maximum torque and motion range of the elbow, wrist, and finger, as listed in Table 1 [29–32]. Due to the large individual differences, we have provided a reference range for the maximum torque. In addition, most studies only refer to fingertip forces; therefore, we calculated the maximum finger torque. Particularly, in the motion range, 0° indicates that the joint is straight, an increasing angle indicates inward flexion, and decreasing angle indicates outward extension. In addition, the motion range of the finger refers to the range reached by the proximal interphalangeal joints. Referring to the actuator model and demand of upper limb motion, the actuator geometrical parameters are listed in Table 2. We first determined the width $2b$ and $2b\prime$ of each joint actuator to fit the human arm and finger dimensions [33, 34]. Other parameters, including the height $2a$, length $2a\prime$, number N, and distance c, were determined considering the actuator shape, angle, and torque requirements. Furthermore, according to tests, the modulus of elasticity of the actuator material is 300 MPa and the Poisson's ratio is 0.256.

Subsequently, we set up an experimental apparatus to characterize the effect of the pressure and initial angle on the actuator flexion/extension torque, as shown in Fig. 4.

Table 1 Needs of flexion and extension for elbow, wrist, and finger

Joint	Maximum torque ($N \cdot m$)	Motion range (°)
Elbow	25–45	0–145
Wrist	5–20	-70–90
Finger	1–4	0–90

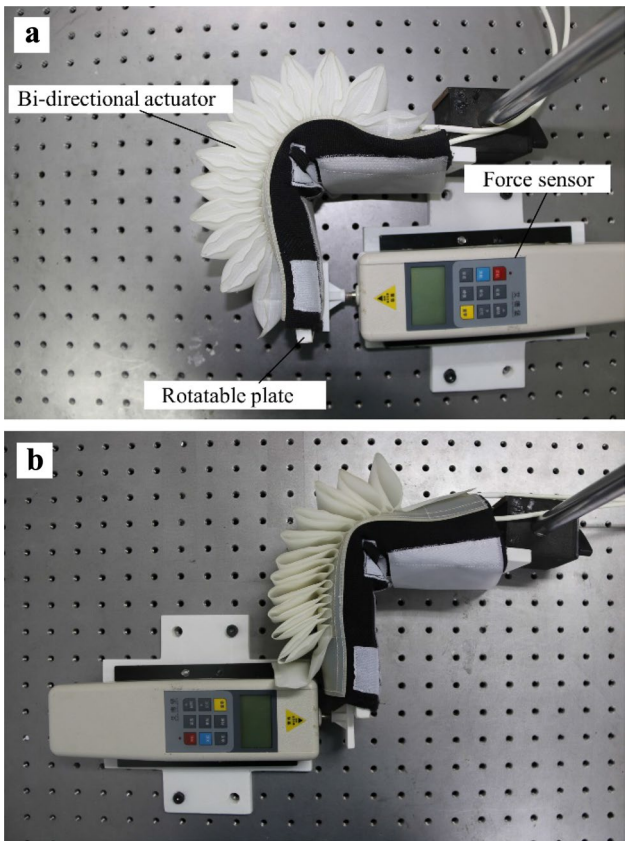

Fig. 4 Characterization of the actuators. **a** Experimental setup for the flexion torque of the actuator. **b** Experimental setup for the extension torque of the actuator

Table 2 Geometric parameters of the bi-directional actuators for elbow, wrist, and finger

	$2a$ (mm)	$2b$ (mm)	c (mm)	N	$2a'$(mm)	$2b'$(mm)
Elbow	40	62	3	24	195	65
Wrist	30	44	2	18	155	50
Finger	20	20	1	12	140	20

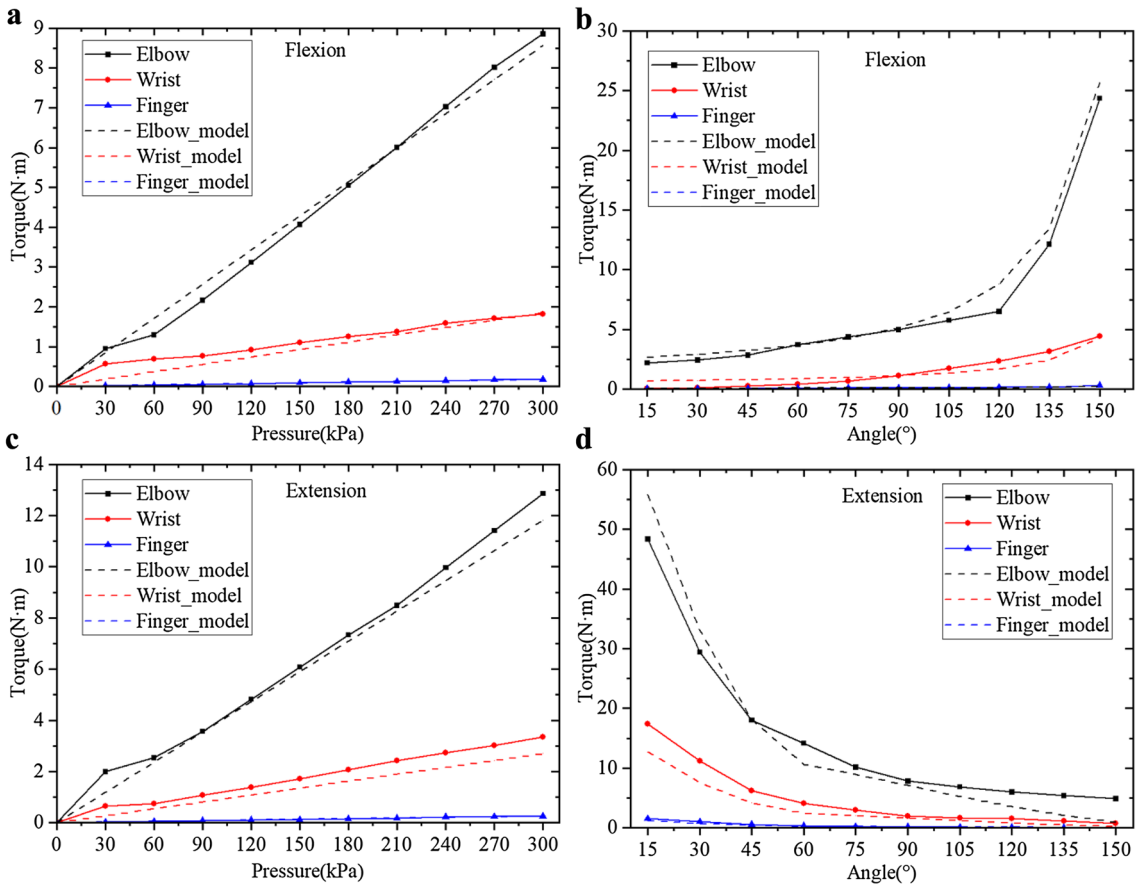

Fig. 5 The characterization of actuators. **a** Effect of input air pressure on the flexion torque of the actuator with 90° angle. **b** Effect of initial bending angle on the flexion torque of the actuator with 180 kPa pressure. **c** Influence of input air pressure on the extension torque of the actuator with 90° angle. **d** Influence of initial bending angle on the extension torque of the actuator with 180 kPa pressure

In the flexion test (Fig. 4a), the initial bending angle θ is set to 90°. The input pressure P increases from 0 to 300 kPa in steps of 30 kPa. The experimental results in Fig. 5a reveal that the torque increases as the pressure increases from 0 to 300 kPa. The elbow, wrist, and finger actuators provide 8.85, 1.82, and 0.18 N · m torque, respectively, when the input pressure is 300 kPa; the corresponding model are 8.57, 1.85, and 0.17 N · m, respectively, which are in good agreement with the experimental results.

In addition, the effect of the initial bending angle on the actuator torque was investigated. A pressure of 180 kPa was maintained during bending. The initial angle was decreased from 150° to 15° in steps of 15°. The experimental results in Fig. 5b show that the torque decreases with the initial bending angle. When the bending angle is 150°, the elbow, wrist, and finger actuators provide torques of magnitudes 24.35, 4.45, and 0.32 N · m, respectively; the corresponding model predictions are 25.65, 4.29, and 0.23 N · m, respectively. The small discrepancy between the model predictions and experimental results is acceptable.

In addition, we tested the extension properties of the actuators, as shown in Fig. 4b. The initial bending angle was set to 90°. The input pressure was increased from 0 to 300 kPa in steps of 30 kPa. The results in Fig. 5c show that the elbow, wrist, and finger actuators provide 12.87, 3.35, and 0.25 N · m extension torques, respectively, at a pressure of 300 kPa; the corresponding model predicted values are 11.81, 2.70, and 0.25 N · m, respectively, which are in good agreement with the experimental results.

Subsequently, we studied the influence of the initial angle on the extension torque. The input pressure is 180 kPa. The initial angle was decreased from 150° to 15° in steps of 15°. The results in Fig. 5d show that the elbow, wrist, and finger

Table 3 Maximum performance of the actuators

Joint	Maximum torque ($N \cdot m$)	Motion range (°)
Elbow	48.35	0–180
Wrist	17.36	0–180
Finger	1.53	0–180

actuators provide extension torques of magnitudes 48.35, 17.36, and 1.53 N · m, respectively; the corresponding model predictions are 55.76, 12.75, and 1.20 N · m, respectively. The discrepancy between the model predictions and experimental results is acceptable.

Finally, we tested the maximum performance of the actuators, including the maximum motion range and torque, as presented in Table 3. The actuators can all be combined head-to-tail. Thus, the cited motion ranges of actuators are 0–180°. Comparing the results with those in Table 1 reveals that the actuator torques satisfy all requirements. The range of motion is slightly insufficient; however, it is adequate for most rehabilitation movements.

3 Soft Robotic Suits

To verify the performance of the actuators on the upper limb assist, we sewed bi-directional actuators on the elastic fabric to create an elbow module, as shown in Fig. 6a-1. As the wrist and hand actuators were close together, we assembled them into a monolithic module, the wrist-hand module, as shown in Fig. 6a-2. The modules were sewn with Velcro and a button for convenience and adaptability.

Further, the modules were integrated into a 3-DOF soft robotic suit with 251 g weight, as shown in Fig. 6b-1. We designed a control box that included power, an air pump, a valve, and a screen. The touchscreen control interface, in Fig. 6b-2, can realize on/off control and force adjustment of different rehabilitation movements. Figure 6c shows various rehabilitation movements of an adult male wearing a soft suit,

Fig. 6 Integration and characterization of the soft robotic suit. **a-1** Elbow module. **a-2** Wrist hand module. **b-1** The suit with integrated modules. **b-2** Control screen. **c** Flexion and extension of elbow, wrist, and finger

such as elbow flexion (c-1), elbow extension (c-2), wrist flexion (c-3), wrist extension (c-4), finger flexion (c-5), and finger extension (c-6).

4 Conclusion and Future Work

This study presents the design, modeling, and characterization of a fabric-based bi-directional actuator for multi-joint flexion/extension. A mathematical model was developed to predict the deformation and output torque of the actuator. Compared with the most existing standard shape assumptions of actuators, we use the large deformation theory to solve the analytic function of the actuator surface. Based on the model and torque requirements, we modify the geometric parameters—without changing the structure—to design and fabricate the elbow, wrist, and finger bi-directional actuator. Finally, we develop a 3-DOF soft robotic suit integrated with the proposed actuator to assist with elbow, wrist, and finger flexion/extensions. Due to the high scalability of the proposed actuator, it is possible to extend assistance to other joints, such as the knee and ankle, by modifying the actuator parameters. In the future, we will explore variable-stiffness actuators to increase the actuator output force and provide a stable variable force for the impedance mode to enhance the rehabilitation training effect. Furthermore, the textile strain sensors will be integrated into the suit to monitor the assisted force and range of motion, achieving self-sensing.

Acknowledgements The research is supported by the National Natural Science Foundation of China (52275002) and the Open Laboratory Concept Verification Project of Zhongguancun National Demonstration Zone (Grant No. 202005226). The authors would like to thank Editage (www.editage.cn) for English language editing.

Data Availability The datasets generated during and/or analyzed during the current study are available from the corresponding author on reasonable request.

Declarations

Conflict of Interest The authors have no competing interests to declare that are relevant to the content of this article.

References

1. Lawrence, E. S., Coshall, C., Dundas, R., Stewart, J., Rudd, A. G., Howard, R., & Wolfe, C. D. (2001). Estimates of the prevalence of acute stroke impairments and disability in a multiethnic population. *Stroke, 32*, 1279–1284. https://doi.org/10.1161/01.str.32.6.1279
2. Ward, N. S., Brander, F., & Kelly, K. (2019). Intensive upper limb neurorehabilitation in chronic stroke: Outcomes from the queen square programme. *Journal of Neurology Neurosurgery and Psychiatry, 90*, 498–506. https://doi.org/10.1136/jnnp-2018-319954
3. Sui, D., Fan, J., Jin, H., Cai, X., Zhao, J., & Zhu, Y. Design of a wearable upper limb exoskeleton for activities assistance of daily living. In *2017 IEEE International Conference on Advanced Intelligent Mechatronics (AIM)*, Munich, Germany, 2017, 845–850.
4. Gonzalez-Mendoza, A., Quinones-Uriostegui, I., Salazar-Cruz, S., Perez-Sanpablo, A. I., Lopez-Gutierrez, R., & Lozano, R. (2022). Design and implementation of a rehabilitation upper limb exoskeleton robot controlled by cognitive and physical interfaces. *Journal of Bionic Engineering, 19*, 1374–1391. https://doi.org/10.1007/s42235-022-00214-z
5. Dragusanu, M., Iqbal, M. Z., Baldi, T. L., Prattichizzo, D., & Malvezzi, M. (2022). Design, development, and control of a hand/wrist exoskeleton for rehabilitation and training. *IEEE Transactions on Robotics, 38*, 1472–1488. https://doi.org/10.1109/tro.2022.3172510
6. Xiloyannis, M., Alicea, R., Georgarakis, A.-M., Haufe, F. L., Wolf, P., Masia, L., & Riener, R. (2022). Soft robotic suits: State of the art, core technologies, and open challenges. *IEEE Transactions on Robotics, 38*, 1343–1362. https://doi.org/10.1109/tro.2021.3084466
7. Lessard, S., Pansodtee, P., Robbins, A., Trombadore, J. M., Kurniawan, S., & Teodorescu, M. (2018). A soft exosuit for flexible upper-extremity rehabilitation. *IEEE Transactions on Neural Systems and Rehabilitation Engineering, 26*, 1604–1617. https://doi.org/10.1109/TNSRE.2018.2854219
8. Butzer, T., Lambercy, O., Arata, J., & Gassert, R. (2021). Fully wearable actuated soft exoskeleton for grasping assistance in everyday activities. *Soft Robotics, 8*, 128–143. https://doi.org/10.1089/soro.2019.0135
9. Xiloyannis, M., Chiaradia, D., Frisoli, A., & Masia, L. (2019). Physiological and kinematic effects of a soft exosuit on arm movements. *Journal of Neuroengineering and Rehabilitation, 16*, 1–15. https://doi.org/10.1186/s12984-019-0495-y
10. Park, Y.-L., Santos, J., Galloway, K. G., Goldfield, E. C., & Wood, R. J. A soft wearable robotic device for active knee motions using flat pneumatic artificial muscles. In *IEEE International Conference on Robotics and Automation (ICRA)*, Hong Kong, China, 2014, 4805–4810.
11. Al-Fahaam, H., Davis, S., Nefti-Meziani, S., & Theodoridis, T. (2018). Novel soft bending actuator-based power augmentation hand exoskeleton controlled by human intention. *Intelligent Service Robotics, 11*, 247–268. https://doi.org/10.1007/s11370-018-0250-4
12. Abe, T., Koizumi, S., Nabae, H., Endo, G., Suzumori, K., Sato, N., Adachi, M., & Takamizawa, F. (2019). Fabrication of "18 weave" muscles and their application to soft power support suit for upper limbs using thin mckibben muscle. *IEEE Robotics and Automation Letters, 4*, 2532–2538. https://doi.org/10.1109/lra.2019.2907433
13. Ge, L., Chen, F., Wang, D., Zhang, Y., Han, D., Wang, T., & Gu, G. (2020). Design, modeling, and evaluation of fabric-based pneumatic actuators for soft wearable assistive gloves. *Soft Robotics, 7*, 583–596. https://doi.org/10.1089/soro.2019.0105
14. O'neill, C. T., Phipps, N. S., Cappello, L., Paganoni, S., & Walsh, C. J. A soft wearable robot for the shoulder: Design, characterization, and preliminary testing. In *2017 International Conference on Rehabilitation Robotics (ICORR)*, London, UK, 2017, 1672–1678.
15. O'neill, C., Proietti, T., Nuckols, K., Clarke, M. E., Hohimer, C. J., Cloutier, A., Lin, D. J., & Walsh, C. J. (2020). Inflatable soft wearable robot for reducing therapist fatigue during upper extremity rehabilitation in severe stroke. *IEEE Robotics and Automation Letters, 5*, 3899–3906. https://doi.org/10.1109/lra.2020.2982861
16. O'neill, C. T., Mccann, C. M., Hohimer, C. J., Bertoldi, K., & Walsh, C. J. (2022). Unfolding textile-based pneumatic actuators for wearable applications. *Soft Robotics, 9*, 163–172. https://doi.org/10.1089/soro.2020.0064
17. Thalman, C. M., Lam, Q. P., Nguyen, P. H., Sridar, S., Polygerinos, P. A novel soft elbow exosuit to supplement bicep

lifting capacity. In *2018 IEEE/RSJ International Conference on Intelligent Robots and Systems (IROS)*, Madrid, Spain, 2018, 6965–6971.
18. Park, S.-H., Yi, J., Kim, D., Lee, Y., Koo, H. S., & Park, Y.-L. A lightweight, soft wearable sleeve for rehabilitation of forearm pronation and supination. In *2019 2nd IEEE International Conference on Soft Robotics (RoboSoft)*, Seoul, Korea, 2019, 636–641.
19. Realmuto, J., & Sanger, T. A robotic forearm orthosis using soft fabric-based helical actuators. In 2019 2nd IEEE International Conference on Soft Robotics (RoboSoft), Seoul, Korea, 2019, 591–596.
20. Bartlett, N. W., Lyau, V., Raiford, W. A., Holland, D., Gafford, J. B., Ellis, T. D., & Walsh, C. J. (2015). A soft robotic orthosis for wrist rehabilitation. *Journal of Medical Devices*. https://doi.org/10.1115/1.4030554
21. Yap, H. K., Khin, P. M., Koh, T. H., Sun, Y., Liang, X., Lim, J. H., & Yeow, C.-H. (2017). A fully fabric-based bidirectional soft robotic glove for assistance and rehabilitation of hand impaired patients. *IEEE Robotics and Automation Letters, 2*, 1383–1390. https://doi.org/10.1109/lra.2017.2669366
22. Proietti, T., O'neill, C., Hohimer, C. J., Nuckols, K., Clarke, M. E., Zhou, Y. M., Lin, D. J., & Walsh, C. J. (2021). Sensing and control of a multi-joint soft wearable robot for upper limb assistance and rehabilitation. *IEEE Robotics and Automation Letters, 6*, 2381–2388. https://doi.org/10.1109/lra.2021.3061061
23. Nassour, J., Zhao, G., & Grimmer, M. (2021). Soft pneumatic elbow exoskeleton reduces the muscle activity, metabolic cost and fatigue during holding and carrying of loads. *Scientific Reports, 11*, 12556. https://doi.org/10.1038/s41598-021-91702-5
24. Ma, J., Chen, D., Liu, Z., & Wang, M. A soft wearable exoskeleton with pneumatic actuator for assisting upper limb. In *IEEE International Conference on Real-time Computing and Robotics (IEEE-RCAR)*, Asahikawa, Japan, 2020, 99–104.
25. Niiyama, R., Sun, X., Sung, C., An, B., Rus, D., & Kim, S. (2015). Pouch motors: Printable soft actuators integrated with computational design. *Soft Robotics, 2*, 59–70. https://doi.org/10.1089/soro.2014.0023
26. Nesler, C. R., Swift, T. A., & Rouse, E. J. (2018). Initial design and experimental evaluation of a pneumatic interference actuator. *Soft Robotics, 5*, 138–148. https://doi.org/10.1089/soro.2017.0004
27. Felt, W. (2019). Folded-tube soft pneumatic actuators for bending. *Soft Robotics, 6*, 174–183. https://doi.org/10.1089/soro.2018.0075
28. Timoshenko, S., & Woinowsky-Krieger, S. (1959). *Theory of plates and shells*. New York: McGraw-hill.
29. Gallagher, M. A., Cuomo, F., Polonsky, L., Berliner, K., & Zuckerman, J. D. (1997). Effects of age, testing speed, and arm dominance on isokinetic strength of the elbow. *Journal of Shoulder and Elbow Surgery, 6*, 340–346. https://doi.org/10.1016/s1058-2746(97)90001-x
30. Pousson, M., Lepers, R., & Van Hoecke, J. (2001). Changes in isokinetic torque and muscular activity of elbow flexors muscles with age. *Experimental Gerontology, 36*, 1687–1698. https://doi.org/10.1016/s0531-5565(01)00143-7
31. Vanswearingen, J. (1983). Measuring wrist muscle strength. *Journal of Orthopaedic & Sports Physical Therapy, 4*, 217–228. https://doi.org/10.2519/jospt.1983.4.4.217
32. Kursa, K., Lattanza, L., Diao, E., & Rempel, D. (2006). In vivo flexor tendon forces increase with finger and wrist flexion during active finger flexion and extension. *Journal of Orthopaedic Research, 24*, 763–769. https://doi.org/10.1002/jor.20110
33. Palatini, P., Fania, C., Ermolao, A., Battista, F., & Saladini, F. (2022). Use of anthropometric indices to identify appropriate cuff shapes for blood pressure measurement: Normative data for adults. *American Journal of Hypertension, 35*, 526–532. https://doi.org/10.1093/ajh/hpac003
34. Hsiao, H., Whitestone, J., Kau, T. Y., & Hildreth, B. (2015). Firefighter hand anthropometry and structural glove sizing: A new perspective. *Human Factors, 57*, 1359–1377. https://doi.org/10.1177/0018720815594933